Cytological Diagnosis Based on Fuzzy Neural Networks

K. Blekas and A. Stafylopatis [*], D. Kontoravdis [†], A. Likas [‡], P. Karakitsos [§]

Abstract

A diagnostic system is presented that employs morphometry combined with a fuzzy neural network approach, for the discrimination of benign from malignant gastric lesions. The input to the system consists of images of routine processed gastric smears stained by Papanicolaou technique. The analysis of the images provided a data set of cell features. The fuzzy min-max neural network classifier, an efficient pattern recognition approach, was used to classify benign and malignant cells based on the extracted morphometric and textural features. The fuzzy min-max classification network is based on hyberbox fuzzy sets and can be incrementally trained requiring only one pass through the training set. The application of the fuzzy min-max neural network yielded high rates of correct classification at both the cell level and the patient level. These results indicate that the use of intelligent computational techniques along with image morphometry may offer very useful information about the potential of malignancy of gastric cells.

1 Introduction

The diagnostic process used in Image Cytometry aims to exploit information extracted from medical images. In usual real life situations, cytopathologists look through the microscope and make a diagnosis probably using a subconscious process based on pattern recognition. Therefore, in practice it is quite difficult

[*] National Technical University of Athens, Department of Electrical and Computer Engineering, 157 73 Zographou, Athens, Greece

[†] 01-Pliroforiki S.A., Athens, Greece

[‡] University of Ioannina, Department of Computer Science, P.O. Box 1186, 451 10 Ioannina, Greece

[§] Department of Clinical Cytology And Cytogenetics, Laiko Hospital, Athens, Greece

to extract and formulate the expert knowledge used by a cytopathologist during diagnosis. The problem in diagnosis is to map the morphometric quantitative descriptions measured to the known qualitative pathological entities.

The application of intelligent computational techniques, such as neural networks and fuzzy systems, seems to provide a solution to the above situation and constitutes a new emerging field in Diagnostic Cytology. Pattern recognition, data base search, knowledge extraction and decision-making, are some of the most important applications of neural networks in the field of Cytology [1, 2, 8, 20]. Up to now neural networks have been successfully applied for the mass screening of Gynaecological Cytology samples [16].

Gastric Cytology has not reached wide acceptance in the investigation of gastric lesions because of the difficulties in the discrimination of benign lesions with severe regenerative alterations from well differentiated cancer cells [9, 12]. However the same diagnostic dilemmas are also present in tissue sections from gastric mucosa biopsies with dysplastic or regenerative changes.

The diagnostic system described here exploits the potential of morphometry combined with fuzzy neural networks in the discrimination of benign from malignant gastric cells in routine prepared gastric smears, in order to explain the difficulties observed by cytopathologists in the interpretation of gastric smears.

Fuzzy min-max neural networks [14, 17, 18] constitute one of the many models of computational intelligence that have been recently developed from research efforts aiming at synthesizing neural networks and fuzzy logic [13, 10, 5].

The fuzzy min-max classification neural network [17] is an on-line supervised learning classifier that is based on *hyperbox* fuzzy sets. A hyperbox constitutes a region in the pattern space that can be completely defined once the minimum and the maximum points along each dimension are given. Each hyperbox is associated with exactly one from the pattern classes and all patterns that are contained within a given hyperbox are considered to have full class membership. In the case where a pattern is not completely contained in any of the hyperboxes, a properly computed fuzzy membership function (taking values in $[0, 1]$) indicates the degree to which the pattern falls outside of each of the hyperboxes. During operation, the hyperbox with the maximum membership value is selected and the class associated with the winning hyperbox is considered as the desicion of the network. Learning in the fuzzy min-max classification network is an *expansion-contraction* process that consists of creating and adjusting hyperboxes (the minimum and maximum points along each dimension) and also associating a class label to each of them. The original definition and operation of the model [17] considers only attributes assuming continuous values. In order to apply the method to pattern recognition problems that involve both discrete and continuous attributes an extension of the model has been developed [14]. To handle discrete attributes, the definition of a hyperbox must be modified to incorporate crisp (not fuzzy) sets in the discrete dimensions.

In the following section the application setup and study design is described. In Section 3 a brief description of the operation and training of the fuzzy min-max classification network is provided. Section 4 provides results from the application of the fuzzy min-max method to the classification of gastric cells. Evaluation of the proposed approach and discussion are provided in Section 5.

2 System Description and Study Design

2.1 System Components

The diagnostic process is complex and can be split into several stages. Figure 1 displays a general schema of the process characterizing the operation of the diagnostic system. It is actually composed of four stages, namely: Image Acquisition, Image Processing, Feature Selection and Classification.

The first stage involves the capturing and analysis of the microscopic images and is very difficult because of the presence of noise and the complexity of the image. The eliminitaion of noise is essential for the cell recognition module. The source of the noise is either the sample itself and/or the miss-calibrated microscope parameters. The process applied for the elimination of noise is median filtering which reduces the image random noise, while keeping all the initial information.

Segmentation of cytoplasm and the cell nuclei is performed during the second stage. To achieve this a suitable preprocessing of the image is applied in such a way that a global threshold based on the histogram can segment the cell nuclei and and the cytoplasm

The characteristics for the discrimination of cells involve two general categories: geometric characteristics and characteristics that are based on individual

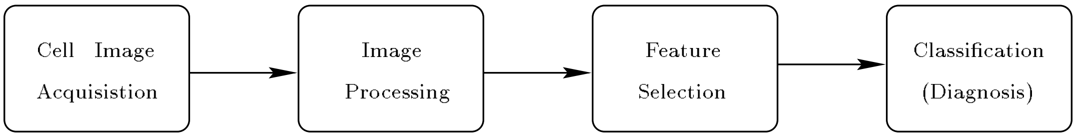

Figure 1: System description

Final diagnosis			
Cytological diagnosis	cancer	gastritis	ulcer
cancer	19		
gastritis		18	
inflammatory displasia			3
true dysplasia	4		
ulcer			24

Table 1: Correlation of Final and Cytological diagnosis

pixel values (optical or density features). The following section provides a more detailed description of the above characteristics. The classification network used in our system is described in Section 3.

The classes in which the cells have been classified varied according to the classification scheme used (see Table 2). Medical applications are very sensitive because they may imply survival or death for humans, so the main target is to perform correct diagnosis for patients and not just cells.

2.2 Specimens and Extracted Features

Sixty eight patients with gastric lesions were investigated in studying the proposed diagnostic approach. The study was performed on brushing cytology smears taken during endoscopy. The smears were routinely fixed in 96^o ethanol for 30 minutes and stained with Papanicolaou technique. The cytological diagnosis was made by at least two cytopathologists with 10 years experience in gastric cytology and was also confirmed by the histologic examination of biopsies and/or surgical specimens. The correlation of the cytological with the final diagnosis is presented in Table 1.

The classes in which the cells have been classified varied according to the classification scheme used (see Table 2). Medical applications are very sensitive because they may imply survival or death for humans, so the main target is to

	5 classes					2 classes	
	Cancer	Gastritis	I-dyspl	T-dyspl	Ulcer	Malignant	Benign
Cells	851	2078	148	171	2685	1022	4911
Patients	19	18	3	4	24	23	45

I-dyspl : Inflammatory dysplasia	Malignant : Cancer and T-dyspl
T-dyspl : True dysplasia	Benign : Gastritis, I-dyspl and Ulcer

Table 2: The data set

perform correct diagnosis for patients and not just cells.

The basic measurements/features that are extracted from every cell can be grouped according to the physical characteristics in two main categories: *geometric* and *densitometric*.

The geometric features are extracted both from the nucleus and the cytoplasm, according to the computational method and the mathematical models reported in the literature [3, 4, ?]. These characteristics describe properties relative to the size (ex. area, perimeter, diameter etc.) or properties that give information about the shape (ex. Form area, Form perimeter etc.) as well as the relative position of the nuclei inside the cell. When the cytoplasm is absent the geometric features of the cytoplasm are considered equal to the geometric features of the nucleus. The feature 'mean radius' of the nucleus is considered as the mean value of the mean radius of all the nuclei included in the cell; for a cell with one nucleus or for a naked nucleus it is considered equal to the mean radius of the nucleus.

Other features that also are extracted are: a) the number of nuclei per cell; if it is a naked nucleus this feature is taken equal to one, b) the mean value of the length of the axes that connect the cell center of mass and the nuclei centers of mass; if it is a naked nucleus this feature has a value of zero (as if one nucleus is in the center of the cell), and finally c) the nucleo-cytoplasmic ratio, which is considered equal to one if the cytoplasm is absent.

The densitometric features provide textural information about nuclei. From the various methods that have been proposed for the description of chromatine texture, it was preferred to implement four models: Histogram, Differences Histogram, Run Length and Co-ocurrence Matrix. The first two models have the advantage of computational simplicity at the cost of poor texture discrimination,

Table 3: Features of data

Type	*Feature*
Geometric for cytoplasm	Areas of Cells
	Circularities of Cells
	Major Axis of Cells
	Minor Axis of Cells
	Perimeter of Cells
	Form area of Cells
	Form perimeter of Cells
	CI of Cells
	Contour Ratio of Cells
	Roundness Factor of Cells
	Diameter of Cells
	Mean Radius of Cells
Geometric for nucleus	Areas of Nuclei
	Circularities of Nuclei
	Major Axis of Nuclei
	Minor Axis of Nuclei
	Perimeter of Nuclei
	Form of Nuclei
	Form perimeter of Nuclei
	CI of Nuclei
	Contour Ratio of Nuclei
	Roundness Factor of Histogram
	Diameter of Nuclei
	Mean Radius of Nuclei in Cell
Densitometric (textural information about nuclei)	Mean of Nuclei Histogram
	Std of Nuclei Histogram
	Var of Nuclei Histogram
	Run Length Short Run of Nuclei
	Run Length Long Run of Nuclei
	Run Length Gray Level of Nuclei
	Run Length Distribution of Nuclei
	Cooccurrence Matrix Maximum of Nuclei
	Cooccurrence Matrix Entropy of Nuclei
	Cooccurrence Matrix Inertia of Nuclei
	Mean of Differences Histogram
	Variance of Differences Histogram
	Contrast of Differences Histogram
	Entropy of Differences Histogram
Other	Nuclei Cytoplasm Ratio
	Nuclei per Cell
	Mean Distance of Nuclei in Cell

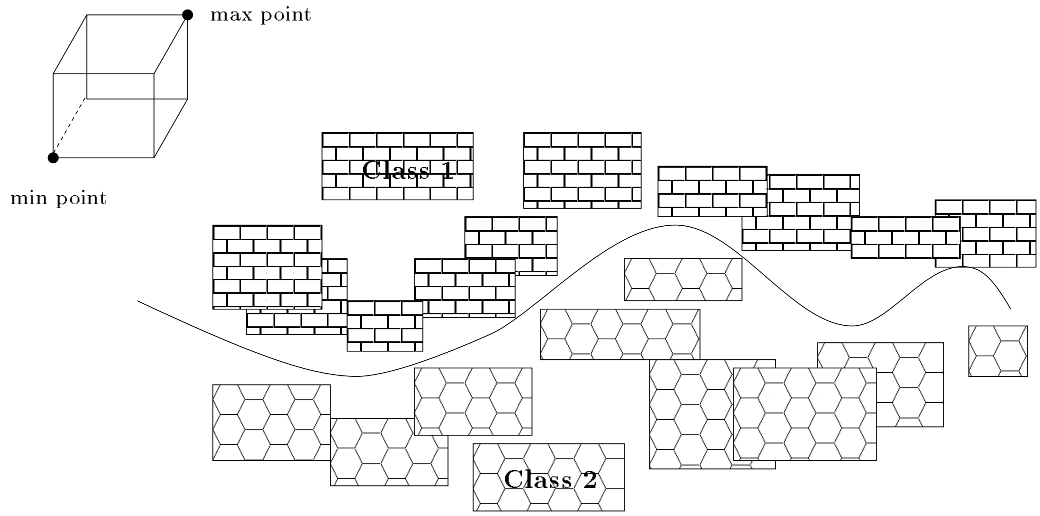

Figure 2: Fuzzy hyperboxes

while the last two models give more precise information on the nuclei structure.

During this study never was a cell encountered with more that one nucleus, so each cell was represented by a vector with 41 elements (12 geometric features for the nucleus, 12 geometric features for the cytoplasm, the number of nuclei, the mean value of the length of the axes that connect the cell center of mass and the nuclei centers of mass, the nucleus cytoplasmic ratio, and 14 densitometric features for the nucleus). These features are shown in Table 3. The descriptive statistics of the features considered are summarised in Appendix A.

3 The Fuzzy Min-Max Classification Network

We have selected a fast and efficient mechanism for the classification part of the diagnostic system, the fuzzy min-max neural network classifier.

The fuzzy min-max neural network is an on-line supervised learning classifier whose operation and training are based on the concept of hyperbox fuzzy sets. Consider a classification problem with n continuous attributes that have been rescaled in the interval $[0,1]$, hence the pattern space is I^n $([0,1]^n)$. Moreover, consider that there exist p classes and B hyperboxes with corresponding minimum and maximum values v_{ji} and w_{ji} respectively ($j=1,\ldots,B$, $i=1,\ldots,n$) (Fig. 2). Let also c_k denote the class label associated with hyperbox B_k.

When the h^{th} input pattern $A_h = (a_{h1},\ldots,a_{hn})$ is presented to the network,

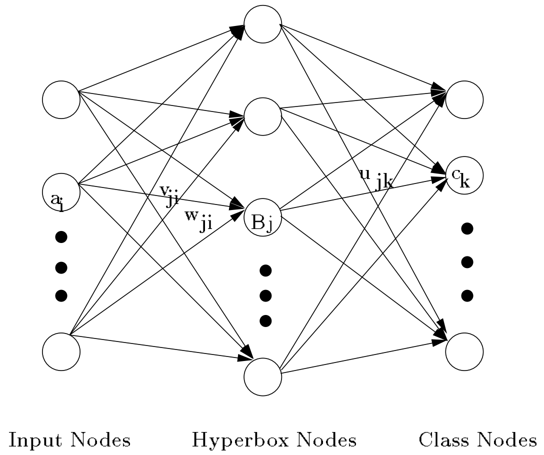

Figure 3: The fuzzy min-max neural network formulation

the corresponding membership function for hyperbox B_j is ([17])

$$b_j(A_h) = \frac{1}{n}\sum_{i=1}^{n}[1 - f(a_{hi} - w_{ji}, \gamma) - f(v_{ji} - a_{hi}, \gamma)] \tag{1}$$

where $f(x, \gamma) = x\gamma$, if $0 \leq x\gamma \leq 1$, $f(x, \gamma) = 1$ if $x\gamma > 1$ and $f(x, \gamma) = 0$ if $x\gamma < 0$. If the input pattern A_h falls inside the hyperbox B_j then $b_j(A_h) = 1$, otherwise the membership decreases and the parameter $\gamma \geq 1$ regulates the decrease rate. As already noted, the class of the hyperbox with the maximum membership is considered as the output of the network.

In a neural network formulation, each hyperbox B_j can be considered as a hidden unit of a feedforward neural network that receives the input pattern and computes the corresponding membership value. The values v_{ji} and w_{ji} can be considered as the weights from the input to the hidden layer. The output layer contains as many output nodes as the number of classes. The weights u_{jk} ($j = 1, \ldots, B$, $k = 1, \ldots, p$) from the hidden to the output layer express the class corresponding to each hyperbox: $u_{jk} = 1$ if B_j is a hyperbox for class c_k, otherwise it is zero. Fig. 3 represents the architecture of the fuzzy min-max classification neural network.

During learning, each training pattern A_h is presented once to the network and the following process takes place: First we find the hyperbox B_j with the maximum membership value among those that correspond to the same class as pattern A_h and meet the expansion criterion:

$$n\theta \geq \sum_{i=1}^{n}(\max(w_{ji}, a_{hi}) - \min(v_{ji}, a_{hi})) \tag{2}$$

The parameter θ ($0 \leq \theta \leq 1$) is a user-defined value that imposes a bound on the size of a hyperbox and its value significantly affects the effectiveness of the training algorithm. In the case where an expandable hyperbox (of the same class) cannot be found, then a new hyperbox B_k is spawned and we set $w_{ki} = v_{ki} = a_{hi}$ for each i. Otherwise, the hyperbox B_j with the maximum membership value is *expanded* in order to incorporate the new pattern A_h, i.e., for each $i = 1, \ldots, n$:

$$v_{ji}^{new} = \min(v_{ji}^{old}, a_{hi}) \tag{3}$$

$$w_{ji}^{new} = \max(w_{ji}^{old}, a_{hi}) \tag{4}$$

Following the expansion of a hyperbox, an *overlap test* takes place to determine if any overlap exists between hyperboxes from different classes. In case such an overlap exists, it is eliminated by a *contraction process* during which the size of each of the overlapping hyperboxes is minimally adjusted. Details concerning the overlap test and the contraction process can be found in [17].

¿From the above description it is clear that the effectiveness of the training algorithm mainly depends on two factors: the value of the parameter θ and the order with which the training patterns are presented to the network.

A basic assumption concerning the application of the fuzzy min-max classification network to a pattern recognition problem is that all attributes take continuous values. Hence, it is possible to define the pattern space (union of hyperboxes) corresponding to each class by providing the minimum and maximum attribute values along each dimension. In the case of pattern recognition problems that are based on both analog and discrete attributes, it is nessecary for the discrete features to be treated in a different way. This results in a modified approach concerning training and operation of the network [14]. In the present study, we have adopted a continuous value representation of features, thus applying the original formulation of the method. Nevertheless, as some features could alternatively be defined as taking values from a discrete domain, the extended model could be used as well.

4 Results

The image analysis part of the system is composed of an IBM compatible Pentium 133MHz computer, equipped with a 1MB Matrox MVP-AT frame grabber and a SONY DXC-151P color CCD camera. The camera is attached to a Nicon Labophot 2 microscope through a C-mount adapter and to the frame grabber by proper cabling. The CCD sensor of the camera has a resolution of 756x581. All images were captured using an objective and digitized to 512x512 pixels.

The software that operates under MS-Windows is used for the segmentation of cells and their nuclei and for the extraction of the measurements that correspond to the features. The S/W is in a high degree customized. A commercially available image processing product is used (OPTIMAS from BioScan Inc.) which supplies a variety of image processing functions and the ability to extract basic geometric and densitometric characteristics from images or parts of images. On the top of this package is applied a library of custom functions. These are written in C (mainly for the segmentation and for texture estimation) and in the macro language that OPTIMAS supports (ALI=Analytical Language for Images) for the user interface, for image storage/retrieval, storage of measurements and for the extraction of texture features.

The study group of our system consisted of data from 68 patients with gastric lesions. Using the custom image analysis described in Section 2, these cases provided a data set of 5933 cells (851 cells from cancer cases, 2078 cells from gastritis, 148 cells from inflammatory dysplasia, 171 cells from true dysplasia, and 2685 ulcer cells respectively). Before entering the data set into the fuzzy neural network classifier they have been normalized to the interval $[0, \ldots, 1]$ for implementation purposes.

In order to evaluate the overal performance of our system four different series of experiment were carried out with respect to the level of examination and the number of classes. We can examine each cell (randomly selected from his/her cell collection), that is the *cellular* level, or the total cells of a patient, that is the *patient* level, so as to indicate the cellular situation of a patient. At the cellular level 1785 cases were used as the training set for the fuzzy min-max neural network classifier, while the rest 4148 cells were used as the testing set. The second experimental series was performed at the patient level where we consider that an input pattern represents one patient. In this case we used the data set of the patients represented by the mean values and the standard deviations of the 68 cases (23 patient cases as training set and 45 as testing set).

Using a different formulation we can divide the above two datasets into ei-

	5 classes					2 classes	
	Cancer	Gastritis	I-dyspl	T-dyspl	Ulcer	Malignant	Benign
Cells	257	626	44	50	808	307	1478
Patients	6	6	2	2	7	8	15

I-dyspl : Inflammatory dysplasia Malignant : Cancer and T-dyspl
T-dyspl : True dysplasia Benign : Gastritis, I-dyspl and Ulcer

Table 4: Training set

	5 classes					2 classes	
	Cancer	Gastritis	I-dyspl	T-dyspl	Ulcer	Malignant	Benign
Cells	594	1452	104	121	1877	715	3433
Patients	13	12	1	2	17	15	30

I-dyspl : Inflammatory dysplasia Malignant : Cancer and T-dyspl
T-dyspl : True dysplasia Benign : Gastritis, I-dyspl and Ulcer

Table 5: Testing set

ther five or two classes. In other words we may represent the problem either as the discrimination of five classes (cancer, gastritis, inflammatory dysplasia, true dysplasia, and ulcer) or as a more coarse classification problem with only two classes: malignant and benign, that can be obtained from the union of the cancer and true dysplasia cases to one class (malignant), and the three other cases to another class (benign).

From the above analysis it is clear that we can examine the performance of our system in four different classification problems. Table 4 shows the training set for the four cases that was randomly composed by selecting 30% of the entire dataset, while Table 5 represents the respective testing set for the same classification problems.

The performance of the fuzzy min-max neural network classifier was evaluated for all four classification cases. The diagrams in Fig. 4 and 5 concern the problems of five classes and two classes respectively and draw up the correct classification rate for cellular level examination. Different values of the parameter θ are considered in the range of $[0.09, \ldots, 0.20]$ with a 0.01 step. For all the obtained rates the number of constructed hyperboxes (B) is also represented. As shown by the diagrams, in the case of five classes the best classification rate was 95.18% and was obtained for the value $\theta = 0.1$, where the neural network

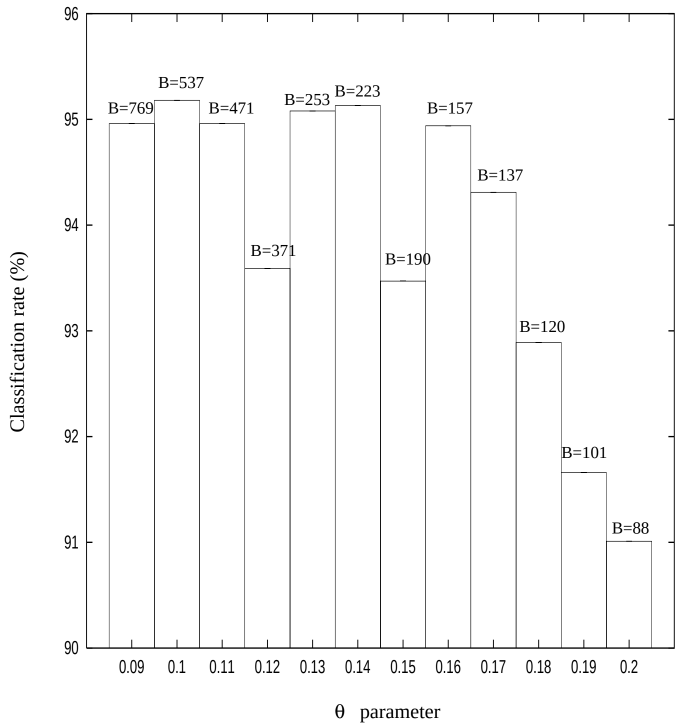

Figure 4: Classification Performance for 5 classes

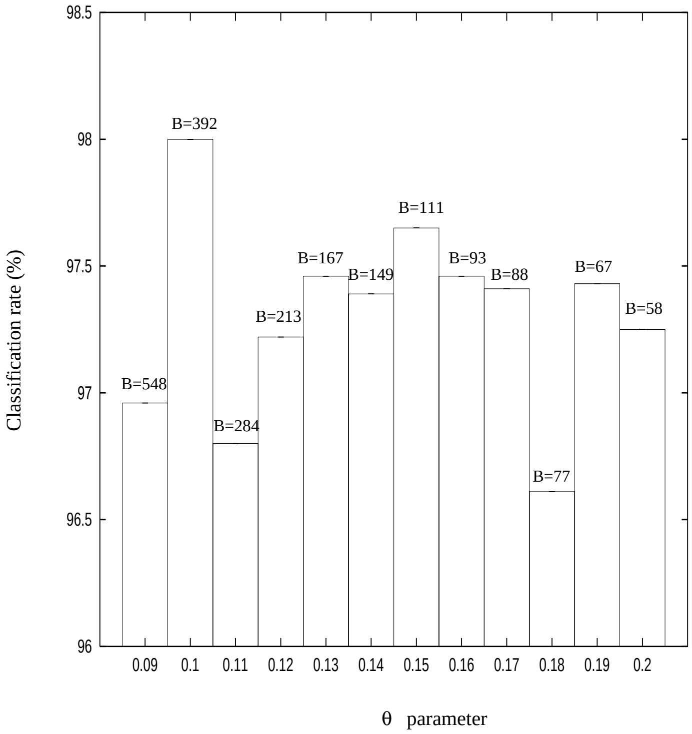

Figure 5: Classification Performance for 2 classes

		Distribution of failure				
	Success	Cancer	Gastritis	I-dyspl	T-dyspl	Ulcer
Cancer	90.74%		65.5%	6.9%	5.2%	22.4%
Gastritis	96.90%	17.8%		11.1%	2.2%	68.9%
I-dyspl	91.35%	11.1%	33.3%		11.1%	44.5%
T-dyspl	56.20%	30.2%	7.5%	20.8%		41.5%
Ulcer	98.14%	20.0%	40.0%	25.7%	14.3%	

Table 6: Percentages of success and failure (cellular level)

constructed 537 hyperboxes. Table 6 illustrates the success rate obtained by the best fuzzy min-max neural network constructed, by providing the classification rate for each of the five cellular classes together with the distribution of misclassified cases. For example, the correct classification rate in the case of cancer is 90.74% and erroneous classification cases are assigned to gastritis at about 65.5%, inflammatory dysplasia at about 6.9%, true dysplasia at about 5.2% and ulcer case at about 22.4%.

Experiments of the two-class problem considering different θ values gave the best classification rate of 98.0% at the value of $\theta = 0.1$ with a network of 392 hyperboxes. The neural network classified the malignant cells with a correct rate of 91.75% while the benign cells were almost perfectly classified (99.30%)

At the patient level the fuzzy neural network classifier was trained and tested in the same manner considering five classes and two classes. In the two cases the network gave a correct classification rate of 93.34% and 97.78% respectively, almost irrespective of the θ values taken in the range $[0.9, \ldots, 0.2]$. The number of constructed hyperboxes was 20 it the case of five classes and 17 in the case of two classes. Considering five classes the network confused only the two dysplasia classes (inflammatory and true) matching them as ulcer class. During the testing operation with two classes (malignant and benign) the neural network responded almost perfectly making only one erroneous diagnosis of malignant class. It must be noted that in all the above experiments the value of parameter g was the same (equal to 2.0).

5 Discussion

Cytology has not reached a wide acceptance in the investigation of gastric lesions because of the relatively high rate of false negative and false positive results. However the same problems may also occur in histologic examination of tissue biopsies [9, 12].

The aim of this study was to investigate the potential role of a diagnostic system in the area of gastric cytology. We have tried to select and propose expert and effective methods in the field of medical analysis and pattern recognition as well as in the selection of features, in order to overcome the difficulties that arise. The diagnostic system is a combination of morphometry with fuzzy neural networks and the objective is to discriminate benign from malignant gastric cells in routine prepared gastric smears.

An important phase of the process was the selection of the data. The features used for our study (see Table 3) were selected beacause they represent classical morphometric and textural characteristics, which correspond to objective estimation of cellular characteristics examined by the eye of a skilled cytopathologist during routine screening. Although the importance of each individual feature is out of the scope of this study, it was decided that several features be extracted from the system as it is accepted that texture gives an indication of the DNA activation, and that changes in the nuclear and cellular size, shape and texture reflect alterations which may be accounted for in the behaviour of the cells.

According to the results, the performance of the fuzzy min-max neural network was excellent in the discrimination of benign from malignant cells. Actually, at the cellular level, the network could discriminate either the five classes or the two general classes with a high success rate. From the results of Table 6 we can extract some significant information about the behaviour and the level of accuracy of our system. The fuzzy neural classifier responds succesfully in the cases of ulcer, gastritis, inflammatory dysplasia and cancer. The low correct classification rate in the case of true dysplasia is very reasonable since this kind of cells corresponds in well differentiated carcinomas ****. When cosidering only two classes (benign, malignant) we obtained higher classification performance, 93.34% of benign and almost 100% of malignant cells. The last rate is very important for cytological diagnosis because it could reduce the uncertainty. At the patient level the results were analogous. Even though the number of data

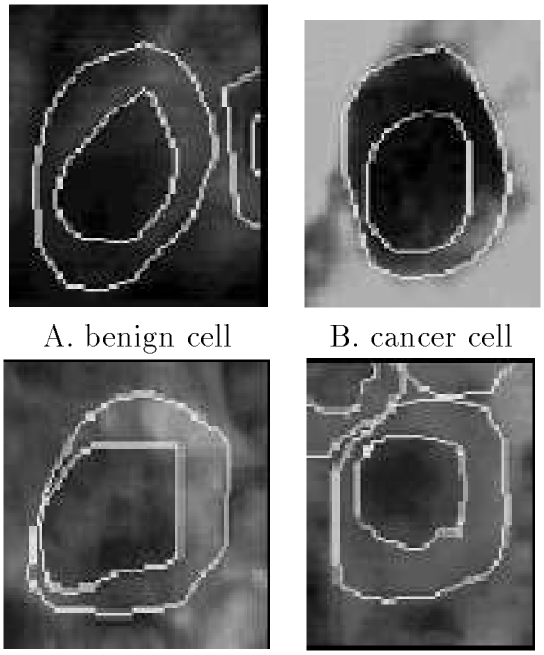

A. benign cell B. cancer cell

C. benign cell D. cancer cell

Figure 6: Sample benign and cancer cells from ulcer cases

available for training was relative small and the number of features was double (adding their standard deviation) the system exhibited an excellent behaviour in both interpretations of classes, making only four and one mistakes respectively.

The failure of the total classification of benign and malignant cells and lesions arises from the fact that in the feature space the borders of the two classes are not always clear. This fact is displayed in Figure 6 showing benign cells from ulcer cases and corresponding cancer cells which are very similar.

Due to the overlap observed in the feature space the discrimination between benign and malignant cells using statistical classifiers has not been succesful, although a statistical significant difference was observed [],[]. The data set used in our experiments has also been used to train a neural network classifier using backpropagation [11]. Although backpropagation exhibited high success rates in the discrimination into two classes, it showed poor performance when it was tested in the classification into 5 classes. Back propagation suffers from the inability to build very efficient descriminated rules for significant cases of data overlapping. Also, it has the disadvantage of requiring a large amount of time to learn the decision boundaries of the classes. On the other hand, the fuzzy min-max neural network classifier bears some desirable features due to the expansion, overlapping test and contraction operations. Thus, it succeeds in determining efficient building blocks (hyperboxes) and eliminating overlapping in the feature space between hyperboxes of different classes, yielding a fast learning operation. Another important advantage in using the fuzzy min-max is that it is robust with respect to the selection of the value of the θ parameter. As can be observed from Fig. 4 and Fig. 5, the classifier shows high classification performance all over the range $[0.09, \ldots, 0.2]$ of θ.

As the experiments indicated, the fuzzy min-max classification neural network constitutes a very promising method for pattern recognition and, more specifically, for medical diagnosis applications. Indeed, through the use of fuzzy logic the system can extract useful information, such as the degree of membership of a cell data to each concerned class. Thus, a cytopathologist may obtain different diagnostic opinions about whether a cell or the collection of a patient's cells belong to each category. Building efficient decision regions and fuzzy geometric structures, the fuzzy min-max neural classifier defines fuzzy internal rules providing a powerful diagnostic tool.

References

[1] M. L. Astion and P. Wilding, "The Application of Back Propagation Neural Networks to Problems in Pathology and Laboratory Medicine," Arch. Pathol. Lab. Med., Vol. 116, pp. 995–1001, 1992.

[2] M. L. Astion and P. Wilding, "Application of Neural Networks to the Interpretation of Laboratory Data in Cancer Diagnosis," Clin. Chem., Vol. 38, No. 2, pp. 34–38, 1992.

[3] J.P.A. Baak, Manual of Quantitative Pathology in Cancer Diagnosis and Prognosis, Springer-Verlag, 1991.

[4] A. G. Baxes, Digital image processing principles and applications, John Wiley, 1994.

[5] K. Blekas, A. Likas and A. Stafylopatis, "A Fuzzy Neural Network Approach Based on Dirichlet Tesselations for Nearest Neighbor Classification of Patterns," Proc. NNASP'95, Boston, MA, Aug. 1995.

[6] M.E. Boon, P.H.J. Kurver, J.P.A. Baak et al., "The Application of Morphometry in Gastric Cytological Diagnosis," Virchows Arch [A] 393, pp. 159–164, 1981.

[7] M. Danno, "Statistical Criteria for the Cytology of Gastric Cancer. A proposal of distance Index," Acta Cytol., Vol. 20, pp. 466–468, 1976.

[8] A. E. Dawson et al., "Nuclear Grading of Breast Carcinoma by Image Analysis," A.J.C.P., Vol. 95, No. 4, pp. 29–37, 1991.

[9] O.A.N. Husain, "Alimentary Tract," pp. 409–432. In Comprehensive Cytology, M. Bibbo (Ed.), Saunders Company, 1991.

[10] IEEE Trans. on Neural Networks, Special Issue on Fuzzy Logic and Neural networks, Vol. 3, No. 5, September 1992.

[11] P. Karakitsos, E. Botsoli Stergiou, A. Pouliakis, M. Tzivras, A. Archimandritis, A. Ioakim Liossi and K. Kyrkou, "The potential of the Back Propagation Neural Network in the Discrimination of Benign from Malignant Gastric Cells," ....

[12] T. Kasugai and S. Kobayashi, "Evaluation of biopsy and Cytology in the Diagnosis of Gastric Cancer," Am. J. Gastrenterol., Vol. 62, pp. 199–203, 1974.

[13] J. Keller and D. Hunt, "Incorporating Fuzzy Membership Functions into the Perceptron Algorithm," IEEE Trans. on Patt. Anal. and Mach. Intell., Vol. 7, pp. 693–699, 1985.

[14] A. Likas, K. Blekas and A. Stafylopatis, "Application of the Fuzzy Min-max Neural Network Classifier to Problems with Continuous and Discrete Attributes," Proc. NNASP'94, Ermioni, Greece, Sept. 1994.

[15] J.M. O'Donoghue, "Adjunctive Endoscopic Brush Cytology in the Detection of upper Gastrointenstinal Malignancy," Acta Cytol., Vol. 39, No. 1, pp. 28–34, 1995.

[16] D. L. Rosenthal and L. J. Mango, "Applications of Neural Networks for Interactive Diagnosis of Anatomic Pathology Specimens," pp. 173–184. In

Compendium on the Computerized Cytology and Histology Laboratory, G. L. Wied et al. (Eds), ToC, Chicago, Illinois, 1994.

[17] P. K. Simpson, "Fuzzy Min-Max Neural Networks-Part 1: Classification," IEEE Trans. on Neural Networks, Vol. 3, No. 5, pp. 776–786, Sept. 1992.

[18] P. K. Simpson, "Fuzzy Min-Max Neural Networks-Part 2: Clustering," IEEE Trans. on Fuzzy Systems, Vol. 1, No. 1, pp. 32–45, Feb. 1993. bibitemSonka94 M. Sonka, V. Hlavac and R. Boyle, Image processing analysis and machine vision, Chapman & Hall, 1994.

[19] P. Tosi, P. Luzi, J.P.A. Baak et al., "Gastric Dysplasia: A stereological and Morphometrical Assessment," J. Pathol., Vol. 152, pp. 83–94, 1987.

[20] H. Truong et al., "Neural Networks as an Aid in the Diagnosis of Lymphocyte-Rich Effusions," Anal. Quant. Cytol. and Histol., Vol. 17, No. 1, pp. 48–54, 1995.

[21] S. A. Zargar, M. S. Khuroo, G. N. Jan, R. Mahajan and P. Shah, "Prospective Comparison of the Value of Brushings Before and After Biopsy in the Endoscopic Diagnosis of Gastroesophageal malignancy," Acta Cytol., Vol. 35, pp. 549–552, 1991.

6 Appendix A

Table 7: Statistics of the data set

Feature	*Class*	*Mean*	*Std*	*Feature*	*Mean*	*Std*
Areas of Cells	Cancer	215.80	202.91	Circularities of Cells	14.31	19.47
	Gastritis	196.28	196.74		4.81	4.82
	I dyspl.	927.99	887.84		5.42	81.61
	T dyspl.	4.33E+3	4285.60		6.22	5.94
	Ulcer	117.282	112.29		845.39	1071.00
Major Axis of Cells	Cancer	19.11	18.76	Minor Axis of Cells	14.58	14.52
	Gastritis	4.03	4.06		2.74	2.76
	I dyspl.	9.94	9.97		7.08	10.59
	T dyspl.	18.29	15.20		8.83	6.94
	Ulcer	5.70	5.49		7.40	8.83
Perimeter of Cells	Cancer	53.52	51.05	Form area of Cells	0.05	2.11
	Gastritis	14.87	14.96		0.50	0.50
	I dyspl.	42.96	34.44		0.02	19.51
	T dyspl.	81.84	73.85		0.00	0.01
	Ulcer	9.25	7.85		24.89	33.02
Form perimeter of Cells	Cancer	0.88	0.84	CI of Cells	3.77	3.63
	Gastritis	0.38	0.38		1.86	1.86
	I dyspl.	0.31	0.03		1.31	0.33
	T dyspl.	-0.07	-0.06		1.47	1.44
	Ulcer	0.01	-0.03		0.42	0.27
Contour Ratio of Cells	Cancer	1.13	1.28	Roundness Factor of Cells	1.06	1.07
	Gastritis	1.39	1.40		1.24	1.24
	I dyspl.	0.41	1.31		0.37	0.41
	T dyspl.	0.80	0.78		0.71	0.70
	Ulcer	1.59	1.55		1.11	1.07
Diameter of Cells	Cancer	15.98	15.11	Mean Radius of Cells	7.91	8.07
	Gastritis	3.01	3.02		1.34	1.35
	I dyspl.	7.19	3.52		2.99	6.68
	T dyspl.	10.20	7.95		4.00	2.91
	Ulcer	1.84	1.33		4.65	4.76
Areas of Nuclei	Cancer	148.53	138.04	Circularities of Nuclei	14.53	15.40
	Gastritis	89.73	89.67		4.74	4.78
	I dyspl.	113.08	105.39		7.54	43.92
	T dyspl.	829.91	811.86		4.11	4.18
	Ulcer	16.02	14.79		204.77	223.10

Table 7: Statistics of the data set

Major Axis of Nuclei	Cancer	15.75	15.47	Minor Axis of Nuclei	12.07	11.72
	Gastritis	3.09	3.09		2.23	2.21
	I dyspl.	4.79	6.78		3.23	6.12
	T dyspl.	7.04	5.79		5.47	4.53
	Ulcer	4.53	4.23		3.96	3.92
Perimeter of Nuclei	Cancer	44.84	42.16	Form area of Nuclei	0.06	1.16
	Gastritis	11.21	11.18		0.46	0.46
	I dyspl.	19.40	16.32		0.02	13.36
	T dyspl.	31.28	27.90		0.02	0.02
	Ulcer	5.12	4.34		13.23	14.37
Form perimeter of Nuclei	Cancer	0.87	0.83	CI of Nuclei	3.80	3.64
	Gastritis	0.39	0.38		1.83	1.84
	I dyspl.	0.32	0.05		1.39	0.42
	T dyspl.	-0.12	-0.12		1.37	1.38
	Ulcer	0.01	-0.02		0.43	0.27
Contour Ratio of Nuclei	Cancer	1.15	1.28	Roundness Factor of Histogram	1.07	1.07
	Gastritis	1.37	1.37		1.21	1.21
	I dyspl.	0.47	1.30		0.39	0.39
	T dyspl.	0.74	0.75		0.70	0.70
	Ulcer	1.57	1.52		1.09	1.05
Diameter of Nuclei	Cancer	13.28	12.49	Mean of Nucleis Histogram	144.39	135.67
	Gastritis	2.36	2.35		233.94	233.56
	I dyspl.	3.63	1.94		424.44	411.35
	T dyspl.	5.70	4.65		519.36	497.73
	Ulcer	1.39	1.14		55.92	53.87
Std of Nucleis Histogram	Cancer	13.14	15.57	Var of Nucleis Histogram	217.20	208.76
	Gastritis	17.82	17.84		2.5E+4	2.5E+4
	I dyspl.	14.05	59.46		7.5E+3	7.4E+3
	T dyspl.	20.04	19.57		1.4E+4	1.4E+4
	Ulcer	183.45	219.80		950.23	943.36
Run Length Sort Run of Nuclei	Cancer	1.9E+4	1.7E+4	Run Length Long Run of Nuclei	0.01	295.43
	Gastritis	8.3E+5	8.3E+5		3.51	3.51
	I dyspl.	1.4E+8	1.3E+7		0.01	8.8E+3
	T dyspl.	2.9E+7	2.9E+7		0.7	0.67
	Ulcer	1.7E+6	1.6E+6		5.5E+6	6.6E+6
Run Length Gray Level of Nuclei	Cancer	3.3E+6	3.0E+6	Run Length Distribu- tion of Nuclei	8.4E+4	8.3E+4
	Gastritis	1.2E+10	1.2E+10		1.4E+7	1.4E+7
	I dyspl.	7.3E+9	7.3E+9		3.4E+6	4.0E+6
	T dyspl.	9.7E+11	9.7E+11		1.9E+9	1.9E+9
	Ulcer	9.2E+8	9.2E+8		1.8E+11	1.9E+11

Table 7: Statistics of the data set

Cooccurrence Matrix Maximum of Nuclei	Cancer	0.00	208.27	Cooccurrence Matrix Entropy of Nuclei	0.001	0.001
	Gastritis	1.66	1.66		1.54	1.54
	I dyspl.	0.00	1.78E+4		0.01	0.01
	T dyspl.	0.61	0.61		0.56	0.56
	Ulcer	3.3E+8	3.3E+8		1.35	1.35
Cooccurrence Matrix Inertia of Nuclei	Cancer	1.82	1.79	Mean of Differences Histogram	18.98	18.28
	Gastritis	6.86	6.92		59.11	59.27
	I dyspl.	17.31	16.41		28.53	23.02
	T dyspl.	33.38	32.51		36.81	37.16
	Ulcer	3.65	3.54		13.48	12.82
Variance of Differences Histogram	Cancer	333.22	325.33	Contrast of Differences Histogram	819.25	805.65
	Gastritis	5.2E+4	5.2E+4		6.8E+5	6.8E+5
	I dyspl.	5.2E+3	5.1E+3		6.3E+4	6.3E+4
	T dyspl.	2.3E+4	2.3E+4		1.5E+5	1.5E+5
	Ulcer	668.07	660.41		1.8E+4	1.9E+4
Entropy of Differences Histogram	Cancer	3.66	31.92	Nuclei Cytoplasm Ratio	0.73	0.87
	Gastritis	1.05	1.05		0.16	0.15
	I dyspl.	1.36	341.50		0.11	1.30
	T dyspl.	0.90	0.90		0.34	0.45
	Ulcer	8.7E+4	8.9E+3		0.79	0.78
Nuclei per Cell	Cancer	1.00	0.96	Mean Distance of Nucleis in Cell	0.28	0.32
	Gastritis	0.22	0.22		0.42	0.42
	I dyspl.	0.33	0.18		0.24	0.43
	T dyspl.	0.25	0.25		-0.33	-0.44
	Ulcer	0.19	0.15		0.24	0.22
Mean Radius of Nucleis in Cell	Cancer	6.57	6.18			
	Gastritis	1.03	1.02			
	I dyspl.	1.54	0.68			
	T dyspl.	2.47	1.95			
	Ulcer	1.36	1.24			